INTERNATIONAL JOURNAL OF PRECISION ENGINEERING AND MANUFACTURING Vol. 14, No. 9, pp. 1667-1675 SEPTEMBER 2013 / 1667
DOI: 10.1007/s12541-013-0226-4

A Review On Active Wind Energy Harvesting Designs

Andrew Truitt[1] and **S. Nima Mahmoodi**[1,#]

1 Department of Mechanical Engineering, The University of Alabama, Box 870276, Tuscaloosa, AL 35487, USA
Corresponding Author / E-mail: nmahmoodi@eng.ua.edu, TEL: 205-348-5056, FAX: 205-348-6419

KEYWORDS: Piezoelectric, Energy harvesting, Wind, Vortex induced vibrations, Bluff bodies, Fluttering, Galloping

This paper aims to review various designs and effects of vibrations generated by fluids, different bluff bodies, aeroelastic instabilities, and study the methods for harvesting their energies by means of piezoelectric materials. Wind based energy harvesting is increasingly pursued due to the ubiquitous nature of excitation source as well as the strong correlation with other types of excitation. Vortex-induced vibrations (VIV), as well as vibrations induced by bluff bodies, and the effect of their own shape on potential gains has been investigated. In addition, the effect of aeroelastic instability phenomenon such as fluttering and galloping on energy generation is investigated. The energy generation density of various methods is evaluated by comparing the gains of different approaches. The study results show that energy densities and peak power outputs vary widely depending on device configuration and instability phenomenon. Additionally, peak power output versus bandwidth varies greatly between the phenomena suggesting specialized applications for a given phenomenon. Through these study results, new research paths to move forward in this field are suggested when paired with the latest examples at active energy harvesting.

Manuscript received: February 06, 2013 / Accepted: June 04, 2013

1. Introduction

The exploration of renewable, sustainable, and green energy resources is currently one of the most critical challenges that we as a society face. In addition to the well known macro-scale resources such as petroleum, coal, hydro-electric, natural gas and nuclear;[1] active research and development is ongoing in the exploration of alternative energy resources such as solar, geothermal, biomass, nuclear (small scale), wind, and hydrogen.[2] On the microscale and nanoscale newer technologies such as piezoelectric energy harvesters are being researched for advanced and upcoming wireless sensor networks, micro-electromechanical devices, and biosensors.[3] Currently, wireless sensor networks[4] are limited by batteries due to inherent economical constraints of replacing hundreds or thousands of batteries. Onsite energy generation would not only save money through the elimination of batteries but also through the elimination of thousands of feet of wiring currently needed for such networks.

As unmanned aerial vehicles (UAV) decrease in size they will require on board energy regeneration to supplement conventional batteries to increase operational time.[5] These quickly developing UAVs are approaching the microscale and someday even the nanoscale scale. A nano-robot, for example, is proposed to be a smart machine that may be able to sense and adapt to the environment, manipulate objects, take actions, and perform complex functions, but a key challenge is to find a power source that can drive the nano-robot without adding much weight.[6] DARPA is testing its next generation of biomimetic microscale UAVs by using insects and their motions as a system model.[7] Green June beetles have been outfitted with piezoelectric generators that harvest energy from wing movement. This has been shown to produce as much as 115 microwatts in optimum conditions and could be sufficient to power future UAVs of similar size.[8] Other examples include implantable medical biosensors that are rapidly becoming commonplace.[9] For nano-systems it is desirable to have on board power generation due to weight, packaging, and servicing requirements. Energy harvesting devices are perhaps best suited to the microscale and nanoscale due to the simple fact that they most often operate most efficiently in the μW to mW range. Power output in this range has been proven to be achievable from piezoelectric energy harvesting systems.[10]

Vibrations are common throughout industrial equipment, cars, planes, boats, and even civil structures.[11-13] Since kinetic energy is derived from motion it follows that the energy generated by kinetic energy harvesting depends on amplitude and type of vibration present. Additionally the efficiency of the generator itself comes into play when discussing coupling; that is to say that the design of the harvester should maximize the coupling effect between the energy source and the transduction mechanism.[14] Thermoelectric, electromagnetic, and piezoelectric are all examples of transduction mechanisms. The yield from the piezoelectric system as well as system configuration (coupling) will vary depending on transduction medium. Piezoelectric transduction uses displacement as the coupling configuration parameter and has been shown to achieve desirable outputs in a variety of applications.[15]

2. Dynamics of Piezoelectric Energy Harvesters

The piezoelectric effect, or the separation of charge within a material as a result of an applied strain, was first discovered by Jacques and Pierre Curie in 1880.[16] They discovered that if certain crystals, such as quartz, were subjected to mechanical strain, they became electrically polarized and the degree of polarization was proportional to the applied strain. Conversely, these materials deform when exposed to an electric field. These effects are illustrated in Figure 1 shown below. Piezoelectric materials come in many forms including high-output single crystals such as PMN-PZT, piezoceramics such as lead zirconate titanate or PZT, bimorph Quick Pack (QP), or Micro Fiber Composites (MFC). Piezoelectric materials typically exhibit anisotropic characteristics, thus, the properties of the material differ depending upon the direction of forces and orientation of the polarization and electrodes. Typically, in the case of piezoelectric films or piezoelectric elements bonded onto substrates, the elements are coupled in the transverse direction. Such an arrangement provides mechanical amplification of the applied stresses. The piezoelectric properties vary with age, stress and temperature.[14]

When modeling the entire dynamic system of a piezoelectric energy harvester one must also consider the dynamics of the piezoelectric actuator. As previously discussed, the piezoelectric effect is an electromechanical phenomenon that occurs when a coupling of electrical and mechanical states occurs due to an applied mechanical stress to dielectric crystals. Conversely, if electrical differential is supplied to the piezoelectric then the system will respond with a mechanical stress in the form of a material deflection. This direct and converse effect makes piezoelectric materials valid for both sensors and actuators. To further understand the operating effects shown in Figure 1, the following coupling equations can be used with the first equation representing the direct effect (i.e., sensing mechanism) while the second equation denotes the converse effect (i.e., actuation mechanism)[18]

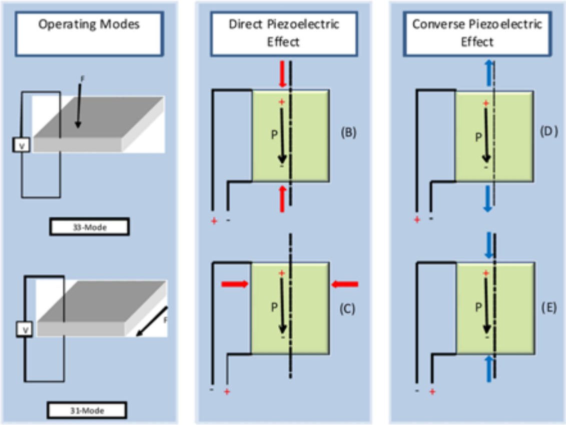

Fig. 1 Illustrated piezoelectric effect[17]

$$S = d_{ij}E + s^{E}T \tag{1}$$

$$D = \varepsilon^{T}E + d_{ij}T \tag{2}$$

where D is the electric displacement (Coulombs/m^2), ε^T is the dielectric constant (permittivity) under constant stress, E is the electric field (V/m), T is stress (N/m^2), d_{ij} is the piezoelectric constant in the ij direction (m/V or Coulomb/N), S is the strain, and S^E is the compliance when the electric field is constant (inverse of the Young's modulus). The different piezoelectric materials can be compared using an electromechanical coupling factor. This factor measures the efficiency of the material to convert mechanical energy into electric energy. The equation to calculate the electromechanical coupling factor is given below

$$k^2 = \frac{d_{33}^2}{s^E \varepsilon^T} = \frac{e_{33}^2}{c^E \varepsilon^T} \tag{3}$$

As discussed with Figure 1 and Equations (1-2), there are different operating effects that are dependent on input. Additionally, there are different operating modes that depend on input. Figure 1 illustrates the 33 and 31 operating modes. In the 33-mode the applied force and subsequent voltage generated act in the same direction. This type of loading typically uses piezoelectric stack-style actuators. Conversely, if piezoelectric bimorph actuators are used, then the 31-mode is utilized. The applied force and generated voltage act perpendicular to one another. It is then clear that not only do the system parameters determine the performance and design of the system, but so too does the choice of operating mode, thereby piezoelectric type, and mounting location. Additionally the sensor itself is subject to nonlinearities due to stress-strain relationship as well as the electromagnetic coupling between the generator and the beam.[19] From a modeling point of view, the actuation force comes through the piezoelectric layer and hence the stress–strain relations are related to actuation voltage and electrical properties of the piezoelectric layer.[20]

A single degree of freedom cantilever style design is one of the most straight forward examples and allows a basic understanding of the governing principles that can be used to understand more complex dynamic systems. The characteristic behavior of a given system can be simplified to two base parameters: damping constant and natural frequency.[18] The mass or lumped mass, spring stiffness, and damping coefficient are represented in variable form by M, K, and C respectively. Energy balanced computational techniques or D'Alembert's principle can be used to derive the equation of motion. The following equation of motion is valid for systems (a) and (b) and follows:

$$M\ddot{z} + C\dot{z} + Kz = -M\ddot{y} \tag{4}$$

where $z = x - y$ is the net displacement of the mass. This can also be rewritten using the two base parameters of damping constant and natural frequency.

$$\ddot{z} + 2\zeta\omega_n\dot{z} + \omega_n^2 x = -\ddot{y} \tag{5}$$

where ζ is the damping ratio and w_n is the natural frequency of the system. The maximum power that can be achieved by the system is

$$P_{\max} = \frac{MY^2\omega_n^3}{4\xi} \tag{6}$$

Maximum power is realized when the natural frequency is the operating frequency. Resonant frequencies of a beam can be determined using the Euler-Bernoulli beam equation. When appropriate end conditions are applied the calculated eigenvalues can be used to find the resonant frequencies of the system.[21] Since the first resonance of a cantilever beam carries the largest amount of energy, harvesters are generally designed to operate in the first resonant mode.[22] The specific derivations of equations of motion for a cantilever design system with proof mass can be found in.[18]

Nonlinear vibrations usually generate high amplitude deformations which provide a better efficiency for energy harvesters. Research into the nonlinearities of piezoelectric dynamic systems has been conducted in reference to Atomic Force Microscope applications,[23] micro cantilevers,[20,24] and active vibration control.[25] Magnetic nonlinearities have also been studied as a way to increase the operating bandwidth of piezoelectric energy harvesters.[26-29] These outcomes, although representative of macro-scale harvesters, can also be applied to micro-scale harvesters. The piezoelectric material can also produce nonlinear terms if the nonlinear constitutive equations are used:[24]

$$D_3 = h_{31}\varepsilon_{11}^p + \beta_{31}Q_3 + \frac{\alpha_3(\varepsilon_{11}^p)^2}{2} + \frac{\alpha_4 Q_3^2}{2} - \alpha_2 Q_3 \varepsilon_{11}^p \tag{7}$$

$$\sigma_{11}^p = E_{31}\varepsilon_{11}^p + h_{31}Q_3 + \frac{\alpha_1(\varepsilon_{11}^p)^2}{2} + \frac{\alpha_2 Q_3^2}{2} - \alpha_3 Q_3 \varepsilon_{11}^p \tag{8}$$

where suffix p is for piezoelectric, E is the modulus of elasticity, v is its Poisson's ratio, Q_3 is the applied electric field, D_3 is the electric displacement, β_{31} is the permittivity coefficient, h_{31} is the piezoelectric constant relating charge density and strain, and the α_i are nonlinear coefficients. The nonlinear equation of motion for a piezoelectric beam including material, geometry, and inertia nonlinear terms can be expressed as[19,30,31]

$$\begin{gathered} m(s)\ddot{v} + (K(s)v'')'' + \left(\frac{3\alpha_1}{2} I_{np}(s) v''^2\right)'' + [v'(K(s)v'v'')']' \\ + \left[v' \int_l^s m(s) \int_0^s (\ddot{v}'v' + \dot{v}'^2) ds\, ds\right] - \left[\frac{1}{2} v'[K_p(s)v'P(t)]'\right]' \\ + \left[\frac{1}{4} K_p(s) v'^2 P(t)\right]'' = \left[\frac{1}{2} K_p(s) P(t)\right]'' \\ v = v' = 0 \quad \text{at } s = 0 \quad v'' = v''' = 0 \quad \text{at } s = l \end{gathered} \tag{9}$$

where $v(t)$ is bending vibration, s is variable along the length of the beam, $m(s)$ is mass density, $P(t)$ is voltage, $K(s)$, $K_p(s)$, and $I_{np}(s)$ are dependent on the physical and geometrical properties of the beam and piezoelectric material.

3. Fluid Based Energy Harvesting: Theories and Principles

Fluid based energy harvesting is a relatively new area of excitation research. As previously discussed, simple impact driven devices were tested, followed by other vibration based systems. These then branched off into other single-degree-of-freedom systems, and finally developed into more complex multi-degree-of-freedom systems. The current methods of fluid based energy harvesting are new technologies that need more investigation and improvement to meet the demands of the rapidly developing micro and nano technology markets. Early experiments were inspired by excessive vibrations due to aerodynamic instability phenomena such as vortex-induced vibration, galloping, flutter and buffeting.[32]

3.1 Vortex Induced Vibrations

Vortex or flow-induced vibrations (VIV) is perhaps one of the more extensively studied methods of fluid based energy harvesting. The driving principle behind this approach is the creation of periodic amplitudes in a body due to periodic cross-wind forces generated by the shedding of vortices in the wake of the given body.[33] Several studies have been performed on VIVs considering the aerodynamic properties and their effects on the system.[34-37] It is continually noted that the Reynolds Number and Strouhal number play significant roles in predicting VIV generation. Current methods do allow for fairly accurate predictions of VIVs, but even the most modern methods are still overly simplified through the elimination of several degrees of freedom. This indicates a great potential for further research in the area.

In one study a harmonica was used as a source of inspiration for the design and analysis.[38] Operation of the harvester begins when wind enters the chamber and tries to escape through the small opening between the cantilever, in this case a reed-like harvester, and the supporting structure. The rapid change in area causes a flow separation from the cantilever at the sharp edge which in turn causes a rapid increase in velocity. This, in turn, produces a pressure drop across the cantilever. This pressure drop deflects the cantilever which increases the aperture area. Consequently, the flow velocity drops and the pressure drop decreases. The mechanical restoring force, or beam elasticity, pulls the beam back decreasing the aperture area and the process is repeated. These periodic fluctuations in the pressure cause the beam to undergo self-sustained oscillations. The resulting periodic strain in the piezoelectric layer produces an electric field via the direct piezoelectric effect which can then be harvested. Figure 2 depicts the device used in this study.

A similar approach with a flow varying pressure chamber has also been studied although the transduction medium in that case was electromagnetic.[40] The proposed Amber Waves of Grain (AWOG) device offers a unique approach of using an array of cantilever piezoelectric beams subject to wind fluid vibrations.[41] While cantilevered designs offer simplified mathematical models, and are often the first models investigated, additional models and computational

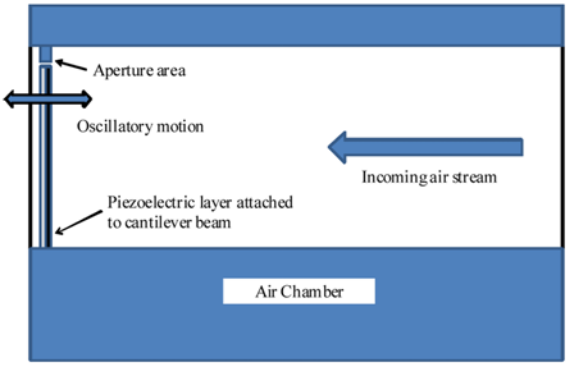

Fig. 2 Schematic of harmonica inspired energy harvester[38]

techniques quickly follow.[42-44] Flexible ceramic cylinders have been subjected to an axial flow that exerts a transverse force on the cylinder due to asymmetrical vortex shedding.[44] This force causes flexural vibrations that are then harvested through piezoelectric generators.

3.2 Bluff Body Effects

The use of bluff bodies to induce vortices is a natural progression of the flow-induced approach and offers advantages in the area of system tuning among others. By placing cantilever beams in the wake of a bluff body vibrations are induced into the structure through vortex shedding. By varying the shape, size, and offset distance of the bluff body the response of the system can be tuned to the natural frequency to obtain maximum energy levels. Furthermore, vortex shedding frequencies in the wake due to the bluff body also depend on parameters such as Reynolds Number, Strouhal Number, and smoothness of the structure.[45] One study analyzed the effects that different bluff body shapes and system parameters have on energy harvesting.[45] In this study a cantilever beam was attached to the trailing edge of the bluff body. The system is fully modeled followed by manipulation of the bluff body shape and its particular influence on lock-in region bandwidth. Lock-in is understood to occur when the frequency of the structure matches that of the undisturbed wake behind the bluff body. Lock-in is of particular significance due to the fundamental importance of frequency matching inherent to energy harvesting as well as the practical problem of fluid flow variations. Realistically, one can expect a fluid flow to be transient and therefore a wideband lock in region is required for any bluff body based energy harvester to be effective. Vortex shedding frequency can be found with the following equation:[45]

$$f_s = \frac{SU}{L} \tag{10}$$

where S is a value assigned for Reynolds number that can vary with bluff body shape, U is flow velocity, and L is the characteristic dimension of the bluff body. While this equation is simple it has profound implications. The conclusion of the study determined that the pentagonal shaped bluff body had the largest lock-in region (Re = 300-1800) but the cylindrical bluff body had the highest average power gain (0.35 mW). Figure 3 shows vortex generation based on different bluff body shapes. It is also worth noting that the study revealed that once lock-in was achieved, (fs = fn) then the free stream velocity could be altered to a degree without detrimental system performance. This is in direct contrast to the next study discussed.

A study of a cylindrical bluff body demonstrated that minor mismatching between the natural frequency of the system and the vortex shedding frequency can have significant detrimental effects on the energy output.[46] This is particularly true when fs < fn for this particular system. This test is visualized through the use of laser sheet illumination in a wind tunnel. Several configurations of the beam in reference to the flow were explored but the highest output was achieved with the beam parallel to the upstream flow in a face-on configuration. In a different approach a cylinder is attached to a hinged splitter plate with piezoelectric elements.[47] The significance of the hinge is that it negates the natural restoring force of the beam found in a system with a rigidly fixed splitter plate. Thus far the experiments presented have focused on aero-elastic interactions. One such example that uses hydrodynamic forces is the energy harvesting eel.[48] As with the previously discussed designs this design also incorporates a bluff body. The main difference is that the fluid in this case is water and the design is developed into a complete system. The purpose was to emulate an eel like life form swimming in a stream or ocean. This is achieved through strips of piezoelectric elements oscillating behind a bluff body complete with on board power storage. A proposed application of this is the powering of oceanographic robots as illustrated in Figure 4.

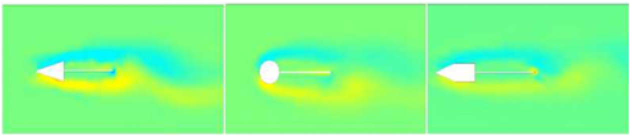

Fig. 3 Vorticity field plot[45]

3.3 Aeroelastic Instabilities and Energy Harvesting

Flutter response is typically categorized as a type of aeroelastic instability. It occurs when there is a positive feedback between the natural frequency of a system and the aerodynamic forces. For flutter, the movement of the object due to vibration increases with aerodynamic load, which in turn drives the object to move further. If the energy input by the aerodynamic excitation in a cycle is larger than that dissipated by the damping in the system, the amplitude of vibration will increase, resulting in self-exciting oscillation. The amplitude can thus build up and is only limited when the energy dissipated by aerodynamic and mechanical damping matches the energy input, which can result in large amplitude vibration and potentially lead to rapid failure.[49] Most flutter based energy harvesters exploit limit cycle oscillations. Cantilevered plates subject to an axial flow show instabilities at sufficiently high flow velocities. When this happens flutter takes place and energy is continually pumped into the plate from the fluid flow while sustaining flutter motion.[50] This critical flutter speed of the system can further be tuned by the damping caused by piezoelectric coupling.[51] Airfoil based designs are particularly interesting examples of flutter response based systems due to the combination of several characteristics previously mentioned.

In one study an airfoil was mounted on a beam with a hinged base.[39] If simply harmonic motion is assumed the following equation can often be used to solve the flutter equation of motion for an airfoil:[52]

$$\left[M_{hh}p^2 + \left(B_{hh} - \frac{\rho c V Q_{hh}^I}{4k}\right)p + \left(K_{hh} - \frac{\rho V^2 Q_{hh}^R}{2}\right)\{u_h\}\right] = 0 \tag{11}$$

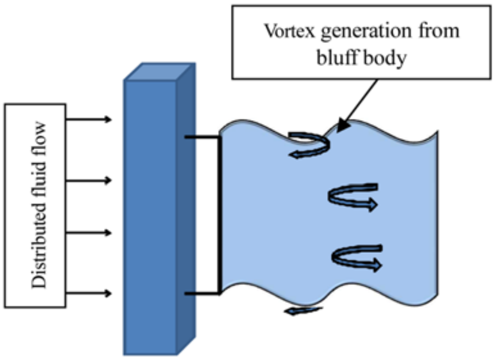

Fig. 4 Model of eel energy harvesting system[48]

where M_{hh} is modal mass matrix, B_{hh} is modal damping matrix, K_{hh} is modal stiffness matrix, Q^I_{hh} is generalized aerodynamic damping matrix, Q^R_{hh} is aerodynamic stiffness matrix, ρ is air density, c is mean aerodynamic chord length, V is airspeed, $k = \omega c/2V$ – reduced frequency, ω is circular frequency, p is $i\omega$, and u_h is modal displacements.

In another study a linearized analytical model is derived which includes the effects of the three-way coupling between the structural, aerodynamic, and electrical aspects of the system. This all contributes to calculations of the wind speed and frequency at the onset of flutter instability. It was determined that a minimum "cut-in" airspeed was needed for the system to operate and such a parameter would need to be taken into design considerations before further system performance characteristics could be tuned to work in the operating range. System nonlinearities are considered in another study as well as linear flutter speed with the particular system achieving 10.7 mW of power output.[53] In addition to the vibrations from fluttering, airfoil systems subject to combined loading with base excitations have also been investigated.[54] Figure 5 is a system model illustrating the various aspects of this system, which is similar to other airfoil system models.

Perhaps unsurprisingly, the output of the harvester is most improved when base excitation frequency matches fluttering frequency. Another consideration though is the base excitations introduced into the host structure from the energy harvester itself.[55] Depending on the nature and size of the host structure any base excitations introduced through the action of the harvester could prove to be severely detrimental through the very same principles upon which the harvester generates energy.

Yet another method of fluid based energy harvesting is the galloping phenomenon. Galloping is an aero-eleastic instability similar to flutter but distinguished by low frequency, large amplitude oscillations of the structure when the direction of the wind excitation is normal to the oscillations.[56] Den Hartog explained the phenomenon for the first time in 1934 and developed a criterion for galloping stability based on specified lift and drag coefficients call the Hartog Factor shown in Equation (12).

$$H(\alpha) = \left(\frac{dC_l}{d\alpha} + C_d\right) > 0 \tag{12}$$

where Cl and Cd are the sectional lift and drag coefficients, respectively, and α is the sectional angle of attack. Galloping occurs at high angles of attack where the aerodynamic coefficients are highly nonlinear. Therefore, the criterion is evaluated by considering a linearized slope of Cl versus α at the equilibrium point about which oscillations occur. Galloping onset is characterized by a negative effective damping of the system and corresponding exponential increase in the amplitude of motion with time. However, the system reaches a limit cycle oscillation in a short period of time, after which the amplitude of oscillation remains constant.[57] Galloping based systems have been shown to develop as much as 50 mW at wind speeds as low as 11.6 mph.[57] The system schematic for such a system is shown in Figure 6.

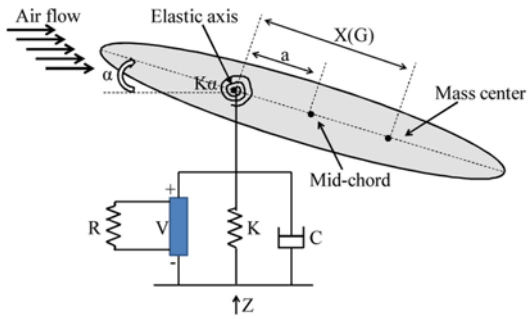

Fig. 5 Schematic diagram of airfoil energy harvester[54]

This approach not only produced more output power than certain flutter designs but also has a lower required air speed. However, there were discrepancies between calculated and experimental, magnitudes and natural frequencies, as well as significant power reductions in the event of high wind velocities. This was attributed to the mass effects of the air and air turbulence. Future works by the author are promised to address these concerns in addition to other concerns such as fatigue life of the device. In another study similar to the optimization of bluff bodies previously mentioned,[45] recent investigations into the optimization of bluff bodies for galloping based harvesters have been investigated as well.[58] The square shape was assumed to be the optimal bluff body shape therefore no other bluff body shapes were investigated in this study. By varying mass, length, and other parameters a maximum

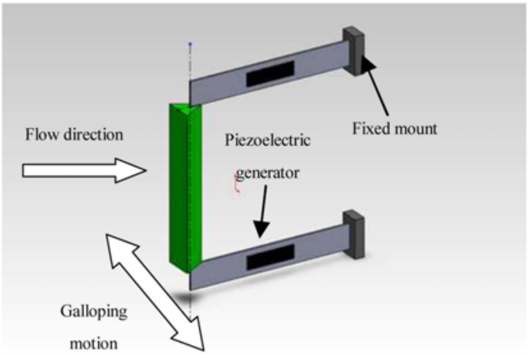

Fig. 6 Schematic for galloping based energy harvester[57]

Table 1 Fluid based piezoelectric energy harvesting output comparison

Fluid Phenomenon	Application	Piezoelectric Element	Maximum Output (μW)	Energy Density (μW/cm^3)	Reference Number
Vortex Induced	Harmonica Chamber	PZT	800	30285	39
Vortex Induced	Wind Tunnel	PZT	7	97	43
Vortex Induced	Wind Tunnel	PVDF	94	158	43
Vortex Induced	Circular Cylinder	PZT	1000	88	46
V.I. with Bluff Body	Cylindrical Bluff Body	PVDF	4	298	47
Fluttering	Pinned Airfoil	PZT	2200	452	39
Galloping	Novel Galloping Structure	PZT	53000	18935	57
Galloping	Optimized Galloping Body	DuraAct piezoceramic	8400	9180	58

output of 8.4 mW was achieved at 8 m/s wind speed. It would be interesting to see the effects of different bluff body shapes on the system as well.

4. Discussion

To further understand the various methods of fluid based energy harvesting it is worth weighing them against one another to better gauge potential advantages currently gained and perhaps yet to be gained. Table 1 lists several works previously mentioned and compares their methods, piezoelectric generator types, energy output, and energy density. The energy density is particularly important as it allows a truer measure of one study and method versus another. It is also worth noting that it is not entirely correct to assume that the method and subsequent experiment with the highest power output is necessarily the best. The end use of the technology will dictate what balance of efficiency, cost, and manufacturability needs to be considered. Several things can immediately be observed when looking at Table 1: First, it appears that there does not seem to be a clear distinction between the use of PVDF and PZT piezoelectric energy harvesters. This depends highly on the application, and in many cases PVDFs are used in fluid excitation due to their increased flexibility over PZTs. This is examined in detail with the direct comparison of both PVDF and PZT harvesters in both wind and water tests.[43] In both cases the PVDF produced a superior output. PZT's do gain an edge over PVDF's though in that they often have higher piezoelectric coefficients. Another observation one could make about the table is that the flutter and galloping based methods produce higher outputs than the vortex induced methods.

While this is true is does come at a cost. They are often limited to a more narrow frequency bandwidth while VIV systems often covers a larger frequency range. In Table 1 the power densities achieved from galloping and fluttering are superior to other methods except for the harmonica chamber example. This gain can be offset by the narrow bandwidth that is sometimes characteristic of aeroelastic based systems. This occurs due to the need to operate galloping and fluttering systems at their natural frequencies. While all systems discussed work best at their natural frequencies it is all but a requirement for galloping and fluttering systems in order to achieve desirable gains. Conversely, mainly vortex based designs will operate within larger bandwidths as discussed previously in the bluff body section.

Currently, the authors are investigation into the use of PVDF as a flag-like harvester. Early results will be briefly discussed but should be considered empirical at best due to excessive turbulence, insufficient testing, etc. The preliminary results do indicate moderate voltage production and will serve as the impetus for future works. The initial test setup is shown in Figure 7. The setup consisted of a hybrid nylon-PVDF piezoelectric harvester, Thor optical table, AC blower fan, and variable frequency drive (VFD). Output voltage was measured directly using an oscilloscope.

Fig. 7 Bench top wind tunnel setup

Testing was conducted at a variety of wind velocities, as measured by an anemometer, and distances from fan to harvester (3, 5, and 7 inches respectively). The harvester was also mounted centered to the flow as well as offset 3 inches. This offset distance was chosen as it was tested to be the shortest offset to instigate change. The results of the combined test are shown in Figure 8.

Testing reveled that voltage production does in fact change with wind velocity as would be expected. However, there do seem to be some nonlinearities as increase velocity does not always equal increased voltage, and the gains and not linear between velocity increases. Additionally, gains vary between centered and offset measurements indicating the potential for system tuning through bluff body or other velocity stream manipulations. Future testing will be conducted in an onsite wind tunnel to improve testing conditions and results. These tests will include a wider range of velocities tested, a wider range of materials tested, bluff body testing, and system modeling.

These pros and cons between different types of piezoelectric harvesters, fluid phenomena, and power management options offer researchers and industries many options moving forward. It is quite possible that applications dictating moderate system deflection, wide operating bandwidth, and higher flow speeds will incorporate VIV based designs using PZT's; while other systems requiring higher degrees of motion, narrower operating bandwidth, and lower flow speeds many incorporate flutter or galloping based designs with PVDF. Numerous other combinations exist in between to suit the given application.

One thing that is shared among all of these types of excitation is the need to improve the power conversion and storage characteristics of the systems. Once the energy is converted by the generator it can be stored and managed in a variety of ways. A simple wave rectifier can be used to convert the AC signal to a DC signal that can then be stored in a

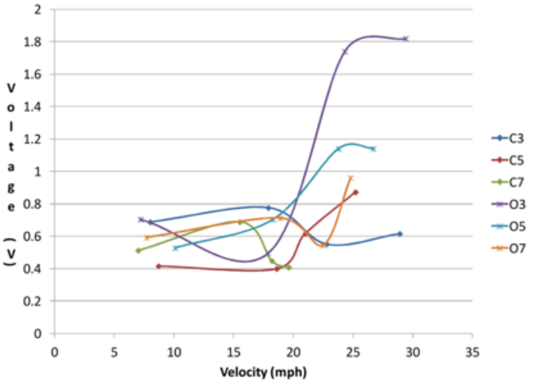

Fig. 8 Voltage vs. wind velocity for bench top test. Centered and Offset data are represented by C and O respectively

capacitor or battery as mentioned earlier. Additionally, Synchronized Switch Harvesting on Inductor or SSHI methods have been compared against a simple resistive load and a rectifier circuit.[59] It was concluded that the SSHI method offered clear gains over other methods and most notably when system coupling was low. Further development of this approach used velocity control rather than the traditional bipolar transistor to effectively create the V-SSHI approach.[60] The device proposed proved to be fully self powered while offering gains of up to 200%.

The final frontier in energy harvesting may in fact be active energy harvesting. In active energy harvesting we are typically monitoring the system through some means and then actively changing the system dynamics in real time to meet changing environmental dynamics. In this way the energy harvester adapts to the environment, stays within its optimum operating range, and generates higher outputs for greater periods of time. One such study uses switch-mode power electronics to control the voltage or charge on the piezoelectric device relative to the mechanical input for optimized energy conversion.[61] This is similar to impedance matching between the system parameters. Power generation was increased by a factor of five compared to traditional rectifier based methods. Another study actually uses a secondary piezoelectric device as a means of system monitoring.[62] The bandwidth was increased by a factor of four. With such substantial gains to be found through active energy harvesting further research should be expected in this area.

5. Conclusion

A brief history into the purpose and potential applications of energy harvesters has been given. Various types of energy harvesting techniques were discussed in which piezoelectric material was chosen as the focal point. Early examples of harvesting techniques were discussed following an introduction into the basics of the piezoelectric principle and its important aspects. Basic dynamics of a piezoelectric system including system nonlinearities were also mentioned. Wind based energy harvesting was then presented as a sub-field of piezoelectric energy harvesting and supported by various fluid based phenomenon. Various methods were compared and contrasted along with the introduction of new work by the author. The power output and density of current studies using PZT piezoelectric harvesters support the notion that they are superior to PVDF-based energy harvesters. However, this author hypothesizes that certain fluid based applications will work best with PVDF-based harvesters and research has begun to investigate this claim. The results from Table 1 also suggest that aeroelastic instability methods are the most dominant fluid forcing phenomena. Energy densities as high as 30.2 mW/cm^3 can be achieved with vortex-induced vibrations but is uncommon at this time. Finally the future of the field in the synergy of active energy harvesting is discussed. It is this author's belief that the developing areas of energy harvesting research will incorporate active control theories and methods in harmony with energy harvesting systems. With continual advancements of the piezoelectric coefficient of materials over time, piezoelectric energy harvesting will further distance itself from other methods of energy harvesting as the dominant form.

REFERENCES

1. Trager, E. C., "Where We Are Now: The U.S. Federal Regulatory Framework for Alternative Energy on the OCS," ASME International Conference on Ocean, Offshore and Arctic Engineering, Vol. 4, pp. 1169-1179, 2009.
2. Holdren, J. P., "Energy and Sustainability," Science, Vol. 315, No. 5813, pp. 737, 2007.
3. Cook-Chennault, K. A., Thambi, N., Bitetto, M. A., and Hameyie, E. B., "Piezoelectric Energy Harvesting: A Green and Clean Alternative for Sustained Power Production," Bull Sci Technol Soc, Vol. 28, No. 6, pp. 496-509, 2008.
4. Enz, C. C., El-Hoiydi, A., Decotignie, J. D., and Peiris, V., "WiseNET: an ultralow-power wireless sensor network solution," Computer, Vol. 37, No. 8, pp. 62-70, 2004.
5. Anton, S. R. and Inman, D. J., "Vibration energy harvesting for unmanned aerial vehicles," Proc. SPIE- Active and Passive Smart Structures and Integrated Systems, Vol. 6928, pp. 692824, 2008.
6. Wang, Z. L., "Energy Harvesting for Self-Powered Nanosystems," Nano Research, Vol. 1, No. 1, pp. 1-8, 2008.
7. Ansari, S. A., Żbikowski, R., and Knowles, K., "Aerodynamic Modelling of Insect-Like Flapping Flight for Micro Air Vehicles," Progress in Aerospace Sciences, Vol. 42, No. 2, pp. 129-172, 2006.
8. Aktakka, E. E., Kim, H., and Najafi, K., "Energy Scavenging from Insect Flight," Journal of Micromechanics and Microengineering, Vol. 21, No. 9, pp. 095016, 2011.
9. Palumbo, A., Amato, F., Calabrese, B., Cannataro, M., Cocorullo, G., Gambarbella, A., Guzzi, P. H., Lanuzza, M., Sturniolo, M., Veltri, P., and Vizza, P., "An Embedded System for EEG Acquisition and Processing for Brain Computer Interface Applications in: Lay-Ekuakille, A. and Mukhopadhyay, S. (Eds.), Wearable and Autonomous Biomedical Devices and Systems for Smart Environment," Springer, pp. 137-154, 2010.
10. Sodano, H. A., Inman, D. J., and Park, G., "Comparison of Piezoelectric Energy Harvesting Devices for Recharging Batteries," Journal of Intelligent Material Systems and Structures, Vol. 16, No. 10, pp. 799-807, 2005.
11. Roundy, S., Wright, P. K., and Rabaey, J., "A Study of Low Level Vibrations as A Power Source for Wireless Sensor Nodes," Computer Communications, Vol. 26, No. 11, pp. 1131-1144, 2003.
12. Ali, S. F., Friswell, M. I., and Adhikari, S., "Analysis of Energy Harvesters for Highway Bridges," Journal of Intelligent Material Systems and Structures, Vol. 22, No. 16, pp. 1929-1938, 2011.
13. Erturk, A., "Piezoelectric Energy Harvesting for Civil Infrastructure System Applications: Moving Loads and Surface Strain Fluctuations," Journal of Intelligent Material Systems and Structures, Vol. 22, No. 17, pp. 1959-1973, 2011.

14. Beeby, S. P., Tudor, M. J., and White, N. M., “Energy Harvesting Vibration Sources for Microsystems Applications,” Measurement Science & Technology, Vol. 17, No. 12, pp. 175-95, 2006.

15. Roundy, S., Leland, E. S., Baker, J., Carleton, E., Reilly, E., Lai, E., Otis, B., Rabaey, J. M., Wright, P. K., and Sundararajan, V., “Improving power output for vibration-based energy scavengers,” IEEE Pervasive Computing, Vol. 4, No. 1, pp. 28-36, 2005.

16. Curie, J. and Curie, P., “Développement, Par Pression, De L’électricit Polaire Dans Les Cristaux Hémièdres Faces Inclinées,” Comptes Rendus De L’Acadeìmie Des Sciences. Seìrie II. Fascicule a, Sciences De La Terre Et Des Planeìtes, 91, pp. 294, 1880.

17. Duran, P. and Moure, C., “Piezoelectric Ceramics,” Materials Chemistry and Physics, Vol. 15, No. 3-4, pp. 193-211, 1986.

18. Jalili, N., “Piezoelectric-Based Vibration Control from Macro to Micro/Nano Scale System,” Springer, 2010.

19. Mahmoodi, S. N., Daqaq, M. F., and Jalili, N., “On the Nonlinear-Flexural Response of Piezoelectrically Driven Microcantilever Sensors,” Sensors and Actuators A: Physical, Vol. 153, No. 2, pp. 171-179, 2009.

20. Mahmoodi, S. N. and Jalili, N., “Non-Linear Vibrations and Frequency Response Analysis of Piezoelectrically Driven Microcantilevers,” International Journal of Non-Linear Mechanics, Vol. 42, No. 4, pp. 577-587, 2007.

21. Braun, S., “Encyclopedia of vibration,” Academic Press, 2002.

22. Roundy, S. and Wright, P. K., “A Piezoelectric Vibration Based Generator for Wireless Electronics,” Smart Materials and Structures, Vol. 13, No. 5, pp. 1131-1142, 2004.

23. Delnavaz, A., Mahmoodi, S. N., Jalili, N., and Zohoor, H., “Linear and Non-Linear Vibration and Frequency Response Analyses of Microcantilevers Subjected to Tip-Sample Interaction,” International Journal of Non-Linear Mechanics, Vol. 45, No. 2, pp. 176-185, 2010.

24. Mahmoodi, S. N., Jalili, N., and Khadem, S. E., “An Experimental Investigation of Nonlinear Vibration and Frequency Response Analysis of Cantilever Viscoelastic Beams,” Journal of Sound and Vibration, Vol. 311, No. 3-5, pp. 1409-1419, 2008.

25. Mahmoodi, S. N., Craft, M. J., and Southward, S. C., “Active Vibration Control using Optimized Modified Acceleration Feedback with Adaptive Line Enhancer for Frequency Tracking,” Journal of Sound and Vibration, Vol. 330, No. 7, pp. 1300-1311, 2011.

26. Stanton, S. C., McGehee, C. C., and Mann, B. P., “Nonlinear Dynamics for Broadband Energy Harvesting: Investigation of a Bistable Piezoelectric Inertial Generator,” Physica D: Nonlinear Phenomena, Vol. 239, No. 10, pp. 640-653, 2010.

27. Mann, B. P. and Sims, N. D., “Energy Harvesting from the Nonlinear Oscillations of Magnetic Levitation,” Journal of Sound and Vibration, Vol. 319, No. 1-2, pp. 515-530, 2009.

28. Stanton, S. C., Mann, B. P., and Owens, B. A. M., “Melnikov Theoretic Methods for Characterizing the Dynamics of the Bistable Piezoelectric Inertial Generator in Complex Spectral Environments,” Physica D: Nonlinear Phenomena, Vol. 241, No. 6, pp. 711-720, 2012.

29. Owens, B. A. M. and Mann, B. P., “Linear and Nonlinear Electromagnetic Coupling Models in Vibration-Based Energy Harvesting,” Journal of Sound and Vibration, Vol. 331, No. 4, pp. 922-937, 2012.

30. Mahmoodi, S. N. and Jalili, N., “Piezoelectrically Actuated Microcantilevers: An Experimental Nonlinear Vibration Analysis,” Sensors and Actuators A: Physical, Vol. 150, No. 1, pp. 131-136, 2009.

31. Mahmoodi, S. N., Jalili, N., and Ahmadian, M., “Subharmonics Analysis of Nonlinear Flexural Vibrations of Piezoelectrically Actuated Microcantilevers,” Nonlinear Dynamics, Vol. 59, No. 3, pp. 397-409, 2010.

32. Duncan, W. J., D. Sc., M. I. Mech. E., F. R. Ae. S., “The Fundamentals of Flutter,” Aircraft Engineering and Aerospace Technology, Vol. 17, No. 2, pp. 32-38, 1945.

33. Jung, H. J. and Lee, S. W., “The Experimental Validation of a New Energy Harvesting System Based on the Wake Galloping Phenomenon,” Smart Materials and Structures, Vol. 20, No. 5, pp. 055022 (10 pp.), 2011.

34. Sarpkaya, T., “A Critical Review of the Intrinsic Nature of Vortex-Induced Vibrations,” Journal of Fluids and Structures, Vol. 19, No. 4, pp. 389-447, 2004.

35. Bearman, P. W., “Understanding and Predicting Vortex-Induced Vibrations,” Journal of Fluid Mechanics, Vol. 634, pp. 1-4, 2009.

36. Williamson, C. H. K. and Govardhan, R., “A Brief Review of Recent Results in Vortex-Induced Vibrations,” Journal of Wind Engineering and Industrial Aerodynamics, Vol. 96, No. 6-7, pp. 713-35, 2008.

37. Williamson, C. H. K. and Govardhan, R., “Vortex-induced vibrations,” Annual Review of Fluid Mechanics, Vol. 36, pp. 413-455, 2004.

38. Bibo, A., Li, G., and Daqaq, M. F., “Electromechanical Modeling and Normal Form Analysis of an Aeroelastic Micro-Power Generator,” Journal of Intelligent Material Systems and Structures, Vol. 22, No. 6, pp. 577-592, 2011.

39. Bryant, M. and Garcia, E., “Modeling and Testing of a Novel Aeroelastic Flutter Energy Harvester,” Journal of Vibration and Acoustics, Vol. 133, No. 1, 2011.

40. Wang, D. A. and Chang, K. H., “Electromagnetic Energy Harvesting from Flow Induced Vibration,” Microelectronics Journal, Vol. 41, No. 6, pp. 356-64, 2010.

41. Sheets, C. and French, J., “Effect Of Geometric and Material Variation of Flow-Induced Micro Energy Harvester for Localized Wind Environments,” Proc. the ASME Conference on Smart Materials, Adaptive Structures and Intelligent Systems, 2012.

42. De Marqui, J. C., Erturk, A., Inman, D. J., and Vieira, W. G. R., "Modeling and Analysis of Piezoelectric Energy Harvesting From Aeroelastic Vibrations using the Doublet-Lattice Method," Journal of Vibration and Acoustics, Vol. 133, No. 1, pp. 011003, 2011.

43. Vatansever, D., Hadimani, R. L., Shah, T., and Siores, E., "An investigation of energy harvesting from renewable sources with PVDF and PZT," Smart Materials and Structures, Vol. 20, No. 5, pp. 055019, 2011.

44. Xie, J., Yang, J., Hu, H., Hu, Y., and Chen, X., "A Piezoelectric Energy Harvester Based on Flow-Induced Flexural Vibration of a Circular Cylinder," Journal of Intelligent Material Systems and Structures, Vol. 23, No. 2, pp. 135-139, 2011.

45. Sivadas, V. and Wickenheiser, A. M., "A study of several vortex-induced vibration techniques for piezoelectric wind energy harvesting," Proc. SPIE Active and Passive Smart Structures and Integrated Systems, Vol. 7977, pp. 79770F, 2011.

46. AkaydIn, H. D., Elvin, N., and Andreopoulos, Y., "Wake of a Cylinder: A Paradigm for Energy Harvesting with Piezoelectric Materials," Experiments in Fluids, Vol. 49, No. 1, pp. 291-304, 2010.

47. Shukla, S., Govardhan, R. N., and Arakeri, J. H., "Flow Over a Cylinder with a Hinged-Splitter Plate," Journal of Fluids and Structures, Vol. 25, No. 4, pp. 713-720, 2009.

48. Taylor, G. W., Burns, J. R., Kammann, S. A., Powers, W. B., and Welsh, T. R., "The Energy Harvesting Eel: a small subsurface ocean/river power generator," IEEE Journal of Oceanic Engineering, Vol. 26, No. 4, pp. 539-547, 2001.

49. Nakamura, Y. and Yoshimura, T., "Flutter and Vortex Excitation of Rectangular Prisms in Pure Torsion in Smooth and Turbulent Flows," Journal of Sound and Vibration, Vol. 84, No. 3, pp. 305-317, 1982.

50. Tang, L., Paidoussis, M. P., and Jiang, J., "Cantilevered Flexible Plates in Axial Flow: Energy Transfer and the Concept of Flutter-Mill," Journal of Sound and Vibration, Vol. 326, No. 1-2, pp. 263-276, 2009.

51. Elvin, N. G. and Elvin, A. A., "The Flutter Response of a Piezoelectrically Damped Cantilever Pipe," Journal of Intelligent Material Systems and Structures, Vol. 20, No. 16, pp. 2017-2026, 2009.

52. Herbert, C., Cowan, D., and Attar, P., "Aerodynamic Flutter Banner," AIAA: Exploring Stuctural Dynamics, 2012.

53. Erturk, A., Vieira, W. G. R., De Marqui, C., and Inman, D. J., "On the Energy Harvesting Potential of Piezoaeroelastic Systems," Applied Physics Letters, Vol. 96, No. 18, pp. 184103, 2010.

54. Bibo, A. and Daqaq, M. F., "Energy harvesting under combines aerodynamic and base excitations," Journal of Sound and Vibration, Vol. 332, No. 20, pp. 5086-5102, 2013.

55. Bryant, M., Tse, R., and Garcia, E., "Investigation Of Host Structure Compliance In Aeroelastic Energy Harvesting," Proc. ASME Conference on Smart Materials, Adaptive Structures and Intelligent Systems, Vol. 2, pp. 769-775, 2012.

56. Chabart, O. and Lilien, J. L., "Galloping of Electrical Lines in Wind Tunnel Facilities," Journal of Wind Engineering and Industrial Aerodynamics, 74-76, pp. 967-976, 1998.

57. Sirohi, J. and Mahadik, R., "Piezoelectric Wind Energy Harvester for Low-Power Sensors," Journal of Intelligent Material Systems and Structures, Vol. 22, No. 18, pp. 2215-2228, 2011.

58. Zhao, L., Tang, L., and Yang, Y., "Small Wind Energy Harvesting From Galloping Using Piezoelectric Materials," ASME Conference on Smart Materials, Adaptive Structures and Intelligent Systems, Vol. 2, pp. 919-927, 2012.

59. Wickenheiser, A. M. and Garcia, E., "Power Optimization of Vibration Energy Harvesters Utilizing Passive and Active Circuits," Journal of Intelligent Material Systems and Structures, Vol. 21, No. 13, pp. 1343-1361, 2010.

60. Chen, Y., Vasic, D., and Costa, F., Wu, W. J., "Self-powered piezoelectric energy harvesting device using velocity control synchronized switching technique," Proc. IECON 36th Annual Conference on IEEE Industrial Electronics Society, pp. 1785-1790. 2010.

61. Liu, Y., Tian, G., Wang, Y., Lin, J., Zhang, Q., and Hofmann, H. F., "Active Piezoelectric Energy Harvesting: General Principle and Experimental Demonstration," Journal of Intelligent Material Systems and Structures, Vol. 20, No. 5, pp. 575-585, 2009.

62. Lallart, M., Anton, S. R., and Inman, D. J., "Frequency Self-Tuning Scheme for Broadband Vibration Energy Harvesting, Journal of Intelligent Material Systems and Structures," Vol. 21, No. 9, pp. 897-906, 2010.